Drift Capacity of Lightly Reinforced Concrete Columns

A Wibowo[1], JL Wilson[1], NTK Lam[2], EF Gad[1,2], M Fardipour[2], K Rodsin[3], P Lukkunaprasit[4],

1) Faculty of Engineering and Industrial Science, Swinburne University of Technology, Hawthorn, 3122, Australia
2) Department of Civil & Environmental Engineering, University of Melbourne, Parkville, 3010, Australia
3) Department of Civil Engineering, King Mongkut's University of Technology, North Bangkok, Thailand
4) Department of Civil Engineering, Chulalongkorn University, Bangkok, Thailand

ABSTRACT

A lightly reinforced column is commonly believed to be relatively brittle with a very low drift capacity. A research project has been undertaken to investigate collapse behaviour of such columns. The effect of variation of axial load ratio and longitudinal reinforcement ratio on flexural, yield penetration, and shear displacement as components of the drift capacity were observed. Interesting outcomes showed that lightly confined reinforced concrete was able to sustain gravity axial load considerably greater than the code recommendations. Moreover, the present shear predictions available are deficient for lightly reinforced columns, since they tend to overestimate the nominal shear strength of the column.

Keywords: Drift capacity, axial load ratio, reinforced column tests, light confinement reinforcement, seismic performance

1 INTRODUCTION

1.1 *Background*

Lightly reinforced concrete columns are prevalent in many old buildings and common in current detailing practice in the regions of lower seismicity. This type of structure is believed to have a very low lateral load and drift capacity from a conventional design perspective. However, many post earthquake investigations (Otani,1997, Wibowo et.al 2008) show that the primary cause of reinforced concrete building collapse during earthquakes is the loss of vertical-load-carrying capacity in critical building components leading to cascading vertical collapse, rather than loss of lateral-load capacity (Ghannoum et.al, 2008).

For example, an existing building may contain an overall weak lateral-force resisting system that is susceptible to shear (point a) and a column that is susceptible to axial failure (point b), as can be seen in Figure 1 (Moehle, 2008). But even though the structure is upgraded by adding new shear walls and hence stiffened and strengthened by the new wall, the building remains vulnerable to loss of vertical-load-carrying capacity if drifts are not controlled to be less than the drift at axial load failure (point b). Therefore, an investigation and laboratory study of non ductile columns has been undertaken to examine the drift capacity and the primary parameters that contribute to the loss of column axial-load capacity.

1.2 *Outline of the paper*

This paper describes the seismic performance assessment of non-ductile columns based on results from laboratory testing. The experimental testing of four column specimens has been undertaken by Swinburne University of Technology in collaboration with The University of Melbourne and Chulalongkorn University. All four columns were subjected to quasi-static cyclic lateral load. The specimens represent some of the most commonly found detailing buildings in developing countries and/or in low-to-moderate seismic regions. These columns are characterized by: moderate aspect ratio, lightly reinforced, limited lateral confinement and moderate axial load ratio.

2 SPECIMEN DESIGN

Four column specimens were designed to represent a prototype of the non-ductile reinforced concrete columns of old buildings in low-to-moderate seismic regions. The two parameters varied were the axial load and longitudinal steel reinforcement ratio. The specimens were 270×300mm cantilever columns with a height (to the application of lateral load) of 1200 mm. All specimens had Grade 500 reinforcing bars with two specimens reinforced with four N12, and the other two specimens reinforced with four N16 (longitudinal reinforcing ratio of 0.56% and 1% respectively). In all cases, R6 stirrups were used at 300mm spacing corresponding to a transverse reinforcement ratio of 0.0007 which is less than minimum lateral reinforcement required by AS3600. All perimeter ties had 135° hooks with just half of the required length of current design codes. The concrete cover was 20mm, whilst the specified concrete compressive strength and steel yield stress were 20 MPa, 536 MPa for main bars and 362 MPa for stirrups, respectively (details are presented in Table 1 and Figure 2).

3 TEST SETUP

The drift capacity of concrete columns is made up of flexural, yield penetration, and shear components which were measured using LVDTs and strain gauges. The axial displacement was also measured to detect loss of axial-load capacity. Displacements were measured using eighteen linear variable displacement transducers (LVDT), as shown in Figure 3a. The arrangement of

LVDT was used in order to measure axial displacement (no. 18), total lateral displacement (no. 1-5), flexural displacement (no. 6-11) and shear deformation (no. 12-17), whilst sixteen strain gauges were installed on the reinforcement to measure the longitudinal and transverse strains (Figures 3b). Three strain gauge locations were used; one level for checking yield penetration length; the second level at the footing-column surface for measuring maximum strain needed for yield penetration; and the third level was at the middle of predicted plastic hinge length.

The axial load was applied and maintained using a hydraulic jack, whilst the lateral load was applied using an actuator with 100 ton loading capacity (Figure 4). The displacement controlled loading sequence consisted of drift-controlled mode at drift increments of 0.25% until reaching 2% drift, and then followed by drift increment of 0.5%. Two cycles of loading were used in each drift ratio to ensure that the hysteretic behaviour could be maintained. Discrete load stages were defined where lateral loading was held constant whilst LVDT and strain gauge measurements were taken, crack patterns recorded, and visual inspections made. The test ended when the column lost the capacity to resist axial load rather than when peak lateral loading capacity of specimen was reduced by 20%.
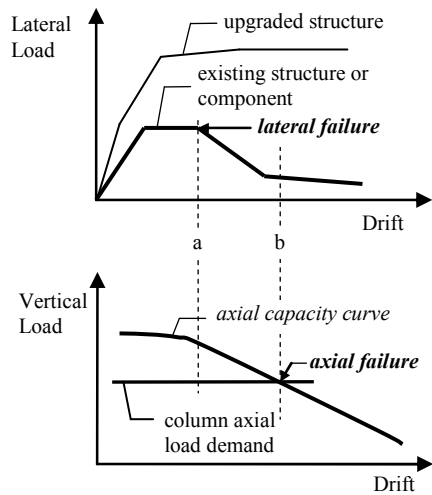

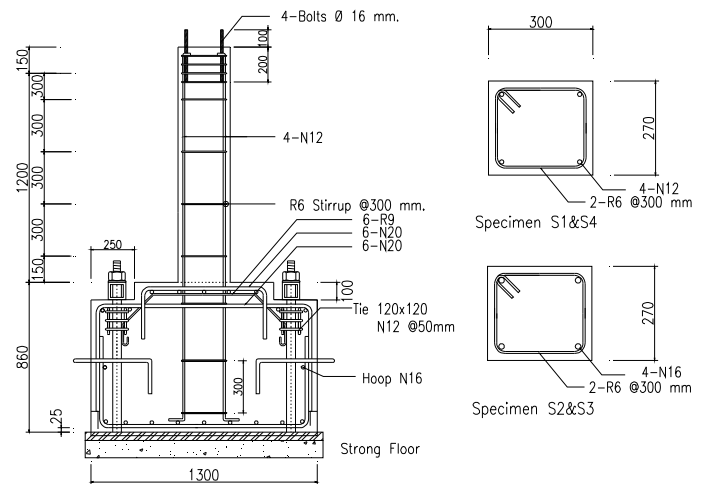Figure 1. Ilustration of strength and deformation demands for existing buildings (Moehle, 2008)

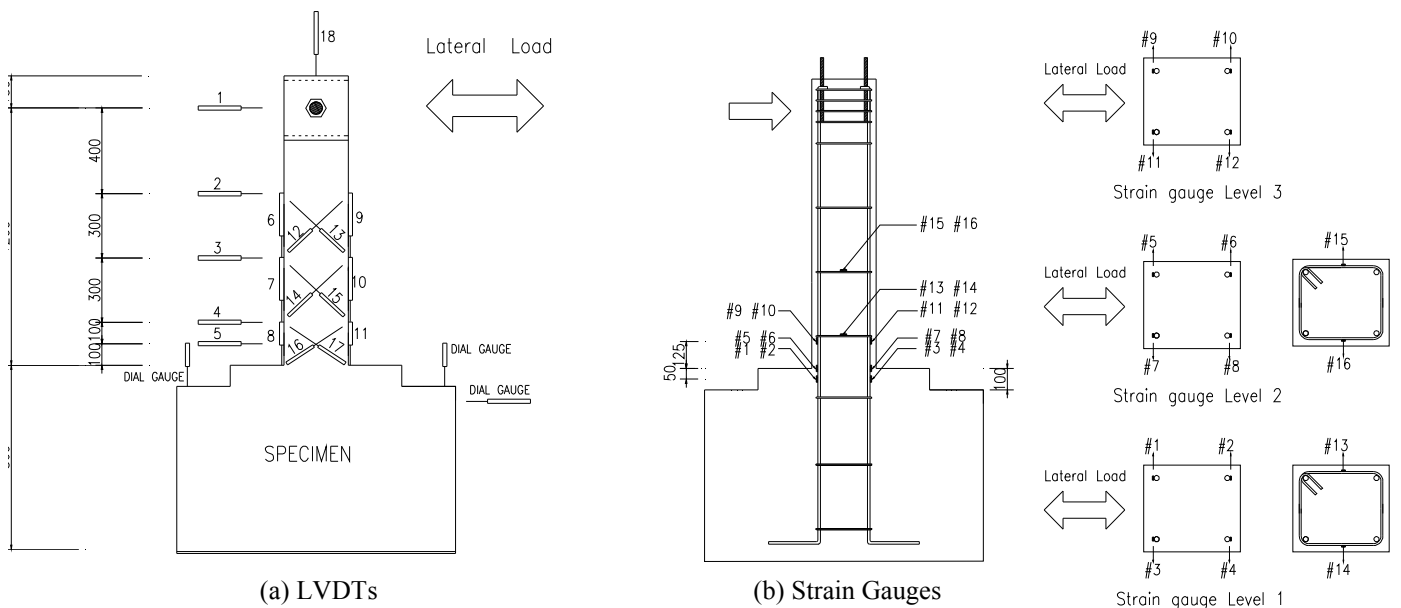Figure 2 Geometry and reinforcement details of column specimens

(a) LVDTs

(b) Strain Gauges

Figure 3 Instrumentation

Table 1 Basic Property of Column Specimens

Spec.	Dimension (mm)	a (mm)	AR	ρ_V	Main Rebar	ρ_H	Ties (@mm)	n	f_c' (MPa)	Hook type
S1	270×300×1200	1200	4	0.56 %	4N12	0.07 %	R6@300	0.2	20.3	135°
S2	270×300×1200	1200	4	1.0 %	4N16	0.07 %	R6@300	0.2	21.0	135°
S3	270×300×1200	1200	4	1.0 %	4N16	0.07 %	R6@300	0.4	18.4	135°
S4	270×300×1200	1200	4	0.56 %	4N12	0.07 %	R6@300	0.4	24.2	135°

Notation : a is shear span which is a clear-height of a column in this case, *AR* is the shear span-to-depth ratio defined as shear span divided by the depth, n is the axial load ratio (ratio of the axial load to axial load-carrying capacity or $A_c f_c'$). ρ_H is the longitudinal reinforcement ratio. ρ_V is the lateral reinforcement (A_{sh}/bs). A_{sh} = total area of transverse reinforcement; s = tie spacing; and b = column section width.
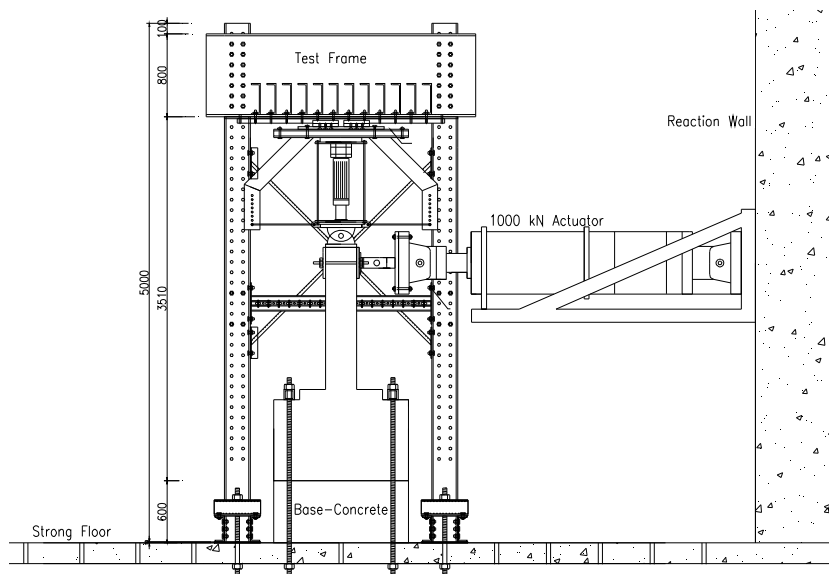

Figure 4 Setup of Loading Test

4   EXPERIMENTAL RESULTS

Specimen S1 with 0.56% rebar ratio and 20% axial load ratio was able to sustain a maximum drift of 5% before gravity load collapse with classical plastic hinge formation at the base of the column and a rigid body rocking mechanism as shown in Figure 5(a). Such desirable behaviour is associated with yield penetration at the base allowing the joint to open and close rather than cracking and spalling of the concrete above the base.

In contrast, specimens S2 and S3 with almost twice the longitudinal reinforcement tolerated lower maximum drifts of 2.5% and 1.5% for axial load ratio of 20% and 40%, respectively. While the analytical formulae predicted flexural failure, the large tie spacing (300 mm) in these specimens lead to buckling of longitudinal bars (ϕ16 mm) and an abrupt transfer of axial load from the steel bars to the concrete. This triggered shear failure due to the deterioration of concrete strength during the cyclic loading as can be seen in Figure 5(b) and 5(c). Meanwhile specimens S4 and S3, both with an axial load ratio of 40% responded in a similar fashion with a maximum drift ratio of 1.5%, despite the different rebar ratio.
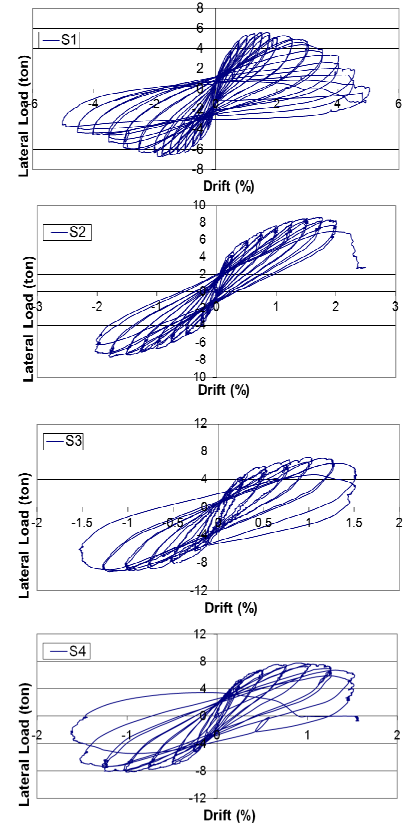
A detailed description of the hysteretic behaviour of all specimens is provided in Wibowo, et.al (2010), whilst an analysis of the components contributing to the drift capacity is presented in the next section.
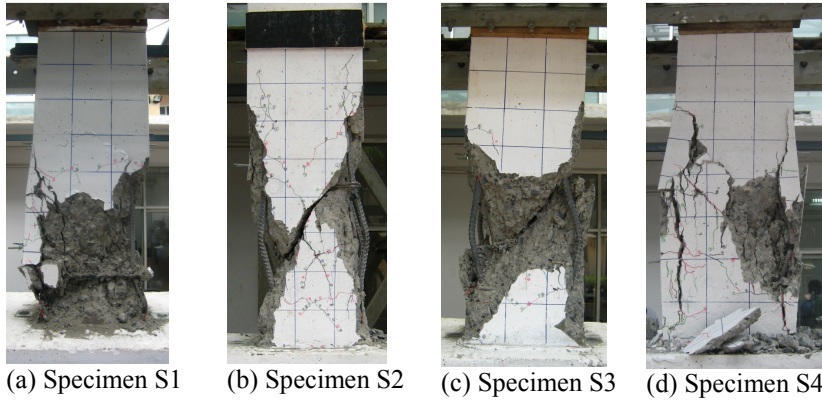
(a) Specimen S1   (b) Specimen S2   (c) Specimen S3   (d) Specimen S4
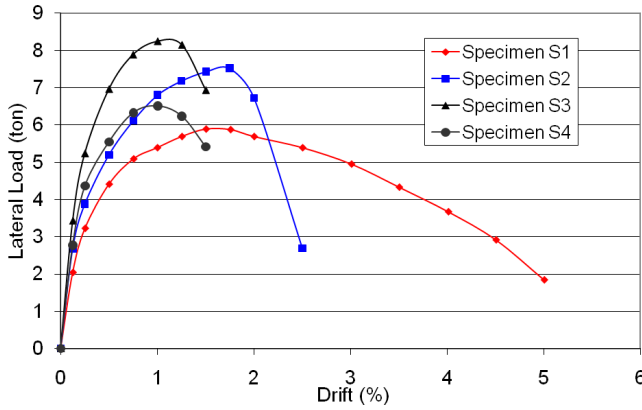
(e) The envelope curve of all specimens (normalized to f_c' 20MPa)

(f) Hysteresis Curve of each specimen

Figure 5 Results of Experiment Test

Table 2 Main Parameters resulted from the test

	S1	S2	S3	S4
Maximum Lateral Load (kN)	59.7	75.1	82.5	63.7
Drift at maximum load (%)	1.71	1.73	1.12	1.01
Lateral load at 80% of peak load (kN)	47.7	60.1	66.0	52
Drift at 80% of peak load (%)	3.3	2.1	1.4	1.5
Axial failure lateral load (kN)	16.1	28.3	50.1	52
Axial failure drift(%)	5.01	2.5	1.5	1.5
Drift ductility	6.68	3.33	1.5	1.5

5 DRIFT COMPONENTS

This section provides drift capacity component measurements based on experimental results. The lateral column displacement can be determined as the sum of the flexural, shear, and yield penetration components. The flexural displacement consists of elastic and plastic components. And the measurement obtained for flexural, shear and yield penetration components can be seen in Figure 6.

5.1 *Flexural Behaviour*

The vertical LVDT (no. 6-11) were used to measure flexural displacement (refer Section 3), where the average curvature of the segment can be estimated via:

$$\varphi = \frac{\beta}{L_V} = \frac{\delta_{f2} - \delta_{f1}}{L_H} \cdot \frac{1}{L_V} \tag{1}$$

where L_v = height per each segment, L_h = distance between flexural LVDTs, δ_f = vertical LVDT measurement.

The top lateral displacement of flexural component for each LVDT segment can be obtained using:

$$\Delta_{fi.i} = \int_0^L \varphi(x)x\,dx = \frac{L - L_{Vi}}{L_H}\left(\delta_{f2} - \delta_{f1}\right) \tag{2}$$

Whilst, the displacement of upper segment without a LVDT transducer can be calculated using

$$\Delta_{fi} = \frac{\varphi L_i^2}{3} = \frac{V L_i^3}{3 E_c I} \tag{3}$$

where V = lateral load; L_i = length of segment.

5.2 Shear Behaviour

The measured shear deformation Δ_{sh} can be estimated from the diagonal LVDT, such that

$$\Delta_{sh} = \frac{(\delta_{s1} - \delta_{s2})}{2}\sec\xi = \frac{(\delta_{s1} - \delta_{s2})}{2}\frac{\sqrt{L_v^2 + D^2}}{L_v} \tag{4}$$

where δ_s = diagonal LVDT measurement, D = cross section depth (parallel to lateral loading direction).

5.3 Yield Penetration Behaviour

The yield penetration effect was obtained from strain gauge and LVDT measurements at the column base interface as shown in Figure 6(c) and showed good agreement. Slip displacement of tensile steel at gap opening can be estimated as follows (Sezen and Moehle, 2003):

$$\text{slip} = \frac{(\varepsilon_{sg1})^2 E_s d_b}{8\sqrt{f_c'}} = \frac{\varepsilon_{sg1} f_s d_b}{8\sqrt{f_c'}} \tag{5}$$

whilst, shortening displacement of compressive steel can be obtained via

$$\delta_{sc} = \varepsilon_{sg2} L_{column} \tag{6}$$

where ε_{sg1} and ε_{sg2} are strain gauge reading at tensile and compressive steel respectively.

Hence, neutral axis depth at column base interface can be estimated via

$$c = (d - d')\frac{\delta_{sc}}{\text{slip} + \delta_{sc}} + d' \tag{7}$$

Slip rotation θ_{slip} is given by

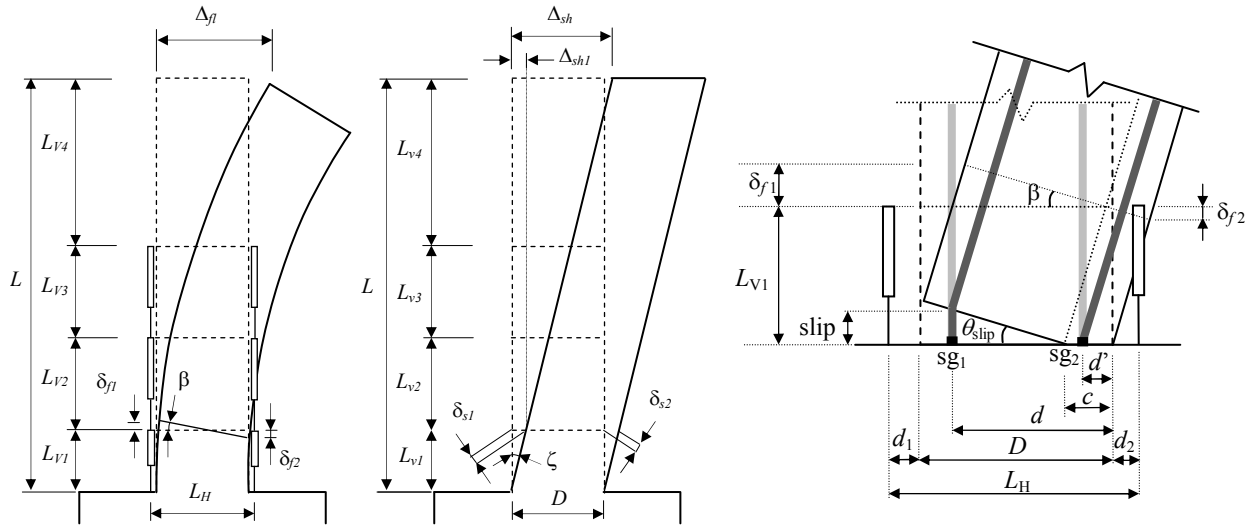$$\theta_{slip} = \frac{\text{slip}}{d - c} \tag{8}$$

Figure 6 Measurement obtained from transducers and strain gauges: (a) flexure, (b) shear, and (c) yield penetration

As a comparison, by assuming a rocking mechanism within the first section of column, an upper bound of slip displacement can be determined from vertical LVDT measurement at the first level (no. 8 and 11) as shown in Figure 6(c). Neutral axis depth at column base interface can be estimated via:

$$c = \frac{\delta_{f2}}{\delta_{f1}+\delta_{f2}} L_H - d_2 \qquad (9)$$

Whilst, the slip rotation of tensile steel can be obtained using:

$$\theta_{slip} = \frac{slip}{d-c} \approx \beta = \frac{\delta_{f2}-\delta_{f1}}{L_H} \qquad (10)$$

Hence, the related slip displacement can be calculated using:

$$slip = \beta(d+d_2)-\delta_{f2} \qquad (11)$$

The top displacement of the column can be calculated from the product of the slip rotation θ_{slip} and the column heights assuming rigid body rotation.

$$\Delta_{yp} = \theta_{slip} L_{column} \qquad (12)$$

5.4 Drift Capacity Assessment

Figure 7 shows the various components of lateral drifts of column for all specimens as a function of lateral load in order to qualitatively indicate the modes of failure. The flexural displacement is presented in two parts, within and outside the predicted plastic hinge length L_p. All specimens show dominant flexural behaviour due to the large aspect ratio of 4, but only specimen S1 ($\rho_v=0.56\%$ and n=0.2) has a concentrated plastic deformation within the predicted plastic hinge length area, whilst the other specimens developed a plastic hinge over a significant length up to the second stirrup. This implies that for non-ductile columns, the standard plastic hinge length predictions developed for ductile columns are inadequate.

Interestingly, specimen S4 ($\rho_v=0.56\%$ and n=0.4) experienced a similar total failure drift capacity compared with S3 ($\rho_v=1.0\%$ and n=0.4), but with different characteristics. S4 responded with a considerable flexural displacement component, whilst the shear component of S3 was

larger. It seems that an increase in the longitudinal reinforcement reduces the flexural component of the total displacement regardless of the value of the total displacement itself.

Displacement due to shear is significant in specimens with higher longitudinal rebar ratio (S2 and S3) since the columns have higher moment capacities and hence higher applied shear forces. On the other hand, the smaller effect of shear deformation in specimen S1 was expected due to the smaller amount of both main rebar ratio and axial load ratio. Overall for all specimens, the increase of axial load ratio resulted in a reduction of total displacement, with a greater reduction for columns with smaller main rebar ratio (compared S1/S4 and S2/S3).

Large yield penetration drift occurred on specimens S1 and S2 due to smaller axial load ratio, with a larger effect on S1 (smaller amount of main reinforcement) compared S2. In contrast, both specimen S3 and S4 experienced only slight yield penetration drift due to the higher magnitude of axial load ratio.
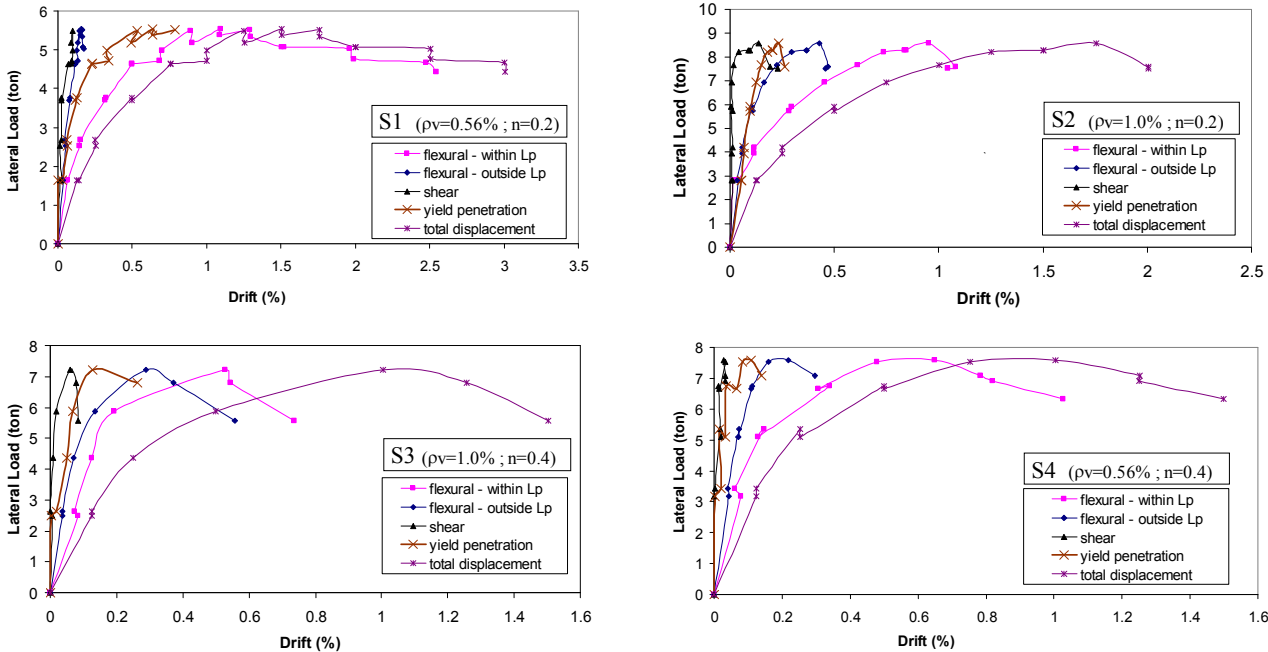

Figure 7 Variation of displacements due to flexure, shear and yield penetration

6 CONCLUSION

Experimental research on non-ductile columns has been undertaken by Swinburne University in collaboration with University of Melbourne and Chulalongkorn University. Four lightly confined concrete columns have been tested with variation of main rebar ratio and axial load ratio parameters. The drift components of flexure, shear and slip and their effect on overall behaviour have been presented in this paper, based on the experimental results.

REFERENCES

FEMA-273. 1997. NEHRP guideline for the seismic rehabilitation of buildings. *Federal Emergency Management Agency*. Washington DC, USA.

Ghannoum, W.M., Moehle, J.P., and Bozorgnia, Y. 2008. Analytical Collapse Study of Lightly Confined Reinforced Concrete Frames Subjected to Northridge Earthquake Ground Motions. *Journal of Earthquake Engineering*, Vol 12, pp 1105–1119.

Lam, S.S.E., Wu, B., Wong, Y.L., Wang, Z.Y., Liu, Z.Q. and Li, C.S. 2003. Drift Capacity of Rectangular Reinforced Concrete Columns with Low Lateral Confinement and High-Axial Load. *Journal of Structural Engineering*, ASCE, Vol. 129(6), pp.733-742.

Moehle, J.P. 2008. Earthquake Collapse Risk of Older Concrete Buildings. *Proc. Luis Garcia Symposium*. Bogota, Colombia, May 2008.

Otani, S. 1999. RC Building Damage Statistics and SDF Response with Design Seismic Forces. *Earthquake Spectra*, Earthquake Engineering Research Institute, Vol. 15, No. 3, pp. 485 - 501.

Priestley, M.J.N., Verma, R., and Xiao, Y. 1994. Seismic shear strength of reinforced concrete column. *Journal of Structural Engineering*, ASCE, Vol. 120(8), pp.2310-2329.

Sezen, H., and Moehle, JP, 2003. Bond-slip behavior of reinforced concrete members, fib-Symposium: Concrete Structures in Seismic Regions, CEB-FIP, Athens, Greece. 2004.

Sezen, H. and Moehle, J.P. 2004. Shear strength model for lightly reinforced concrete columns. *Journal of Structural Engineering*, ASCE, Vol. 130(11), pp. 1692-1703.

Wibowo A, Wilson JL, Gad EF, and Lam NTK. 2010. Collapse Modelling Analysis of a Precast Soft-Storey Building in Melbourne. *Engineering Structural Journal*, Elsevier. Special Issue: Learning Structural Failures, Vol. 32(7), July, pp 1925-1936.

Wibowo A, Wilson JL, Fardipour M, Lam NTK, Rodsin K, Lukkunaprasit P, Gad EF. 2010. Seismic Performance Assessment of Lightly Reinforced Concrete Columns. *Procs. Of Australasian Conference on the Mechanics Structures and Materials*, Melbourne, Australia, 7-10 December, paper no. 68.

Wibowo, A., Kafle, B., Kermani, A.M., Lam, N.T.K, Wilson, J.L., Gad, E.F. 2008. Damage in the 2008 China Earthquake. *Procs. of Australian Earthquake Engineering Society Conference*, Ballarat, Australia, 21-23 November.